Our reference: YPREP 3981 P-authorquery-v8

AUTHOR QUERY FORM



Journal: YPREP

Article Number: 3981

Please e-mail or fax your responses and any corrections to:

E-mail: corrections.essd@elsevier.sps.co.in

Fax: +31 2048 52799

Dear Author,

Please check your proof carefully and mark all corrections at the appropriate place in the proof (e.g., by using on-screen annotation in the PDF file) or compile them in a separate list. To ensure fast publication of your paper please return your corrections within 48 hours.

For correction or revision of any artwork, please consult http://www.elsevier.com/artworkinstructions.

Any queries or remarks that have arisen during the processing of your manuscript are listed below and highlighted by flags in the proof. Click on the 'Q' link to go to the location in the proof.

Location in article	Query / Remark: <u>click on the Q link to go</u> Please insert your reply or correction at the corresponding line in the proof
<u>Q1</u>	Please confirm that given names and surnames have been identified correctly.
<u>Q2</u>	Please check the fax number of the corresponding author, and correct if necessary.

Highlights

► APPTM has been successfully overexpressed as a fusion protein with MBP. ► Pure APPTM can be obtained by Ni-NTA chromatography, TEV protease cleavage and RP-HPLC. ► Isotopically labeled APPTM WT and an FAD mutant were purified for NMR studies. ► Excellent HSQC spectra were obtained in DPC and SDS micelles.

FISEVIER

Contents lists available at SciVerse ScienceDirect

Protein Expression and Purification

journal homepage: www.elsevier.com/locate/yprep



25

27

29

30

32

33

34

35

36

37

38 39

58

60

61

62

63

64 **65**

66

67

68

69

70

71

72

73

74

75

76

78

83

Expression, purification, and reconstitution of the transmembrane domain of the human amyloid precursor protein for NMR studies

4 Q1 Wen Chen¹, Eric Gamache¹, Panielle Richardson, Zhenming Du, Chunyu Wang^{*}

Department of Biology, Center for Biotechnology and Interdisciplinary Studies, Rensselaer Polytechnic Institute, 110 8th Street, Troy, NY 12180, United States

6 7

ARTICLE INFO

Article history:

Received 14 June 2011

and in revised form 8 August 2011

3 Available online xxxx

4 Keywords:

15 Alzheimer's disease

16 Amyloid precursor protein (APP)

17 Membrane protein

Transmembrane domain

19 APPTM

20 HSQC

23

42

43

44 45

46

47

48

49

50

51

52

53 54

55 56

21 Micelle

γ-Secretase

ABSTRACT

Alzheimer's disease (AD) is the most common type of dementia in elderly people. Senile plaques, a pathologic hallmark of AD, are composed of amyloid β peptide (A β). A β aggregation produces toxic oligomers and fibrils, causing neuronal dysfunction and memory loss. A β is generated from two sequential proteolytic cleavages of a membrane protein, amyloid precursor protein (APP), by β - and γ -secretases. The transmembrane (TM) domain of APP, APPTM, is the substrate of γ -secretase for A β production. The interaction between APPTM and γ -secretase determines the production of different species of A β . Although numerous experimental and theoretical studies of APPTM structure exist, experimental 3D structure of APPTM has not been obtained at atomic resolution. Using the pETM41 vector, we successfully expressed an MBP-APPTM fusion protein. By combining Ni-NTA chromatography, TEV protease cleavage, and reverse phase HPLC (RP-HPLC), we purified isotopically-labeled APPTM for NMR studies. The reconstitution of APPTM into micelles yielded high quality 2D 15 N- 1 H HSQC spectra. This reliable method for APPTM expression and purification lays a good foundation for future structural studies of APPTM using NMR.

© 2011 Elsevier Inc. All rights reserved.

Introduction

Alzheimer's disease $(AD)^2$ is the most common type of dementia in elderly people [1]. One of the pathologic hallmarks of AD, senile plaque, is mainly composed of amyloid β peptide $(A\beta)$. The length of the $A\beta$ peptide usually ranges from 39 to 43 residues. The two major isoforms of $A\beta$ in the brain are $A\beta$ 40 and $A\beta$ 42, consisting of 40 and 42 residues respectively [2,3]. While $A\beta$ 40 is relatively benign, $A\beta$ 42 tends to aggregate rapidly into neurotoxic oligomers and fibrils (plaques) [4]. $A\beta$ is produced from the amyloid precursor protein (APP) through two sequential proteolytic cleavages by β - and γ -secretases [5].

APP is a membrane protein with a single transmembrane (TM) domain (APPTM). The proteolytic cleavage of APP is initiated by β -secretase within the extracellular domain of APP, releasing a C-terminal membrane-anchored fragment of 99 residues (C99) [6,7], C99 is further cleaved by γ -secretase within the TM domain to yield A β and the APP intracellular domain (AICD) [8–10].

However, the cleavage of C99 by γ -secretase within the TM domain is not specific. Several cleavage sites have been identified, and A β peptides of varying length can be generated during γ -secretase cleavage. A β 40 is predominantly released from the TM domain cleavage, and A β 42 is generated to a lesser extent [4].

APPTM is the substrate of γ -secretase for the production of A β and the interaction between APPTM and γ -secretase is crucial for γ -secretase specificity, that is, the preference of A β 40 production over A β 42 production. Familial Alzheimer's disease (FAD) is caused by missense mutations in genes encoding γ -secretase and APP. FAD mutations within APPTM alter γ -secretase specificity and lead to an increased A β 42/A β 40 ratio [11,12]. Therefore, there is tremendous interest in obtaining the 3D structure of APPTM at atomic resolution and in understanding how the specifics of the structure may contribute to γ -secretase specificity.

Beel et al. [13] presented the first solution NMR studies of C99, which includes APPTM, and characterized the cholesterol binding properties of C99. However, due to the large size of the system (C99 + detergent micelle), complete side chain assignment, a prerequisite for NMR structure determination, was not achieved. Using a limited number of distance constraints from solid state NMR and molecular dynamics (MD) simulation, Sato et al. [14] obtained a structural model for APPTM. Computational models for APPTM have also been generated by Miyashita et al. [15], and recently Wang et al. [16]. To date, there is still no experimental 3D structure of APPTM at atomic resolution based on large numbers of distance and angular constraints.

 $1046\text{-}5928\slash\!\!/\,^s$ - see front matter @ 2011 Elsevier Inc. All rights reserved. doi:10.1016/j.pep.2011.08.006

Please cite this article in press as: W. Chen et al., Expression, purification, and reconstitution of the transmembrane domain of the human amyloid precursor protein for NMR studies, Protein Expr. Purif. (2011), doi:10.1016/j.pep.2011.08.006

^{*} Corresponding author. Fax: +1 518 276 3497. E-mail address: wangc5@rpi.edu (C. Wang).

¹ These two authors made equal contributions to this paper.

² Abbreviations used: AD, Alzheimer's disease; APP, amyloid precursor protein; TM, transmembrane domain; APPTM, transmembrane domain of APP; MBP, maltose binding protein; HPLC, high performance liquid chromatography; AAA, quantitative amino acid analysis; SDS, sodium dodecyl sulfate; DPC, dodecylphosphocholine; HSQC, Heteronuclear Single Quantum Coherence; TEV, tobacco etch virus.

100

110

119 120 121

118

141

142

143

144

To simplify the NMR spectra for structure determination, we have decided to pursue a smaller construct composed only of APPTM sequence, which was shown to be an excellent substrate for γ -secretase [17]. We started with APPTM with the V44M FAD mutation (V44 is named in according to A β numbering). We expressed recombinant APPTM V44M in <code>Escherichia coli</code> cells using the pETM41 vector (EMBL Protein Expression and Purification Facility). pETM41 uses maltose-binding protein (MBP) as the fusion partner which can increase expression level, stability and solubility. The His-tag at the N-terminus can be used for affinity purification. A TEV protease recognition site is present between MBP and APPTM, which is crucial for the release of APPTM from the MBP fusion protein. After successful expression using pETM41, we purified APPTM V44M and WT with isotopic labeling for NMR studies. Good HSQC spectra of APPTM WT and V44M have been obtained in DPC and SDS micelles.

Materials and methods

$Construction\ of\ APPTM\ expression\ vector$

Codon optimized DNA of human APPTM mutant V44M was synthesized and cloned into the pZERO-2 vector by Integrated DNA Technologies (IDT). The DNA flanked with NcoI and BamHI restriction sites was digested and ligated into the NcoI and BamHI sites in the pETM41 vector, which encodes kanamycin resistance. After completion of cloning from pZERO-2 to pETM41, the DNA of pETM41-APPTM V44M was verified by DNA sequencing. The resulting plasmid encodes an N-terminally hexahistidine-tagged fusion protein of MBP and APPTM, with a TEV protease recognition site in between. The final APPTM V44M sequence after purification and TEV protease cleavage will be GAMAKGAIIGLMVGGVVI-ATMIVITLYMLKKK (the site of mutation M44 is in bold), which contains 28 residues from APP, and 4 additional residues at the N-terminus (underlined in the sequence), which are leftover from the cloning process and recognition site of the protease. pETM41-APPTM WT was then obtained using the DNA Quickchange kit (Stratagene) and confirmed by DNA sequencing.

Expression and purification of APPTM

The pETM41-APPTM plasmid was transformed into E. coli BL21 (DE3) cells on kanamycin plates. A single colony was picked and used to inoculate an overnight 100 ml culture in LB broth (Sigma) at 37 °C with shaking at 250 rpm. Overnight culture was then used to start expression to make natural abundant proteins in 2 LB broth at 37 °C at a starting OD₆₀₀ of 0.1. After OD₆₀₀ reaches 0.3, the cells were cold shocked on ice for 30 min. Isopropyl-thio-galactoside (IPTG) was then added to the culture to 1 mM to initiate expression. Optimal expression was obtained when cell culture was then shaken at 250 rpm at 30 °C for 24 h. Cells were harvested by centrifugation at 8000g at 4 °C for 30 min. Cell pellets were stored at -80 °C prior to protein purification. 15N-labeled proteins were prepared from M9-based minimal medium containing ¹⁵NH₄Cl Cells were then resuspended in lysis buffer (50 mM sodium phosphate, 200 mM NaCl, 5 mM imidazole, and 10 mM β-mercaptoethanol, pH 7.4) plus protease inhibitor cocktail for His-tagged proteins (Sigma). Cells were lysed on ice by sonication using 45% power with 10 cycles of 20 s on and 30 s off. Cell lysate was then mixed with 1% Triton-X 100 and rocked on Nutator for 20 min at 4 °C. Lysate was separated into a soluble fraction and inclusion bodies via centrifugation for 30 min at 37,500g at 4 °C. The soluble fraction was loaded onto a 5 ml HisTrap HP column (GE Healthcare) which was pre-equilibrated with 5 column volumes of equilibration buffer (50 mM sodium phosphate, 200 mM NaCl, 5 mM imidazole, pH 7.4). The HisPrep column was run on an AKTA FPLC purification system

(Amershan Biosciences) using a flow rate of 1.5 ml/min. The column was first washed with 2 column volumes of equilibration buffer, followed by a single linear gradient of 0–500 mM imidazole in elution buffer (50 mM sodium phosphate, 200 mM NaCl, 500 mM imidazole, pH 7.4) over 10 column volumes. The column was then washed with 6 column volumes of elution buffer. Four milliliter fractions were collected and MBP fusion protein-containing fractions were identified by SDS-PAGE. These fractions were combined and dialyzed (20,000 MWCO) into to exchange TEV protease digestion buffer (50 mM Tris-HCl, 0.5 mM EDTA, 30 mM NaCl, 1 mM DTT, pH 8.0), and the concentration of the fusion protein should be kept <3 mg/ml to avoid aggregation and precipitation. Bradford assay was used to determine fusion protein yield. Each mg of fusion protein was then digested with 0.2 mg TEV protease at room temperature for up to 48 h. Efficiency of digestion was tested by SDS-PAGE. Solid urea (Sigma) was added to 6 M to stop the reaction and help solubilize APPTM. The reaction mixture was the spun down at 20,000g for 5 min. The supernatant was injected onto a reverse phase C4 HPLC column (Grace Discovery) (250 mm in length, 9.4 mm in diameter, 5 μm particle size, and 300 Å pore size). APPTM was finally purified by HPLC (Shimadzu) with a linear gradient of 40-100% of buffer B (90% acetonitrile, 0.1% trifluoroacetic acid) over buffer A (10% acetonitrile, 0.1% trifluoroacetic acid) in 40 min with a flow rate at 3 ml/min. The identity and purity of APPTM was confirmed with MALDI mass spectrometry (Bruker). APPTM in acetonitrile/water solvent was frozen and lyophilized. APPTM powder was stored at −20 °C until further use.

145

146

147

148

149

150

151

152

153

154

155

156

157

158

159

160

161

162

163

164

170

171

172

173

174

175

176

177

178

179

180

181

182

183

184

185

186

187

188

190

191

192

193

194

195

196

197

198

199

200

201

Reconstitution of APPTM into membrane mimics

¹⁵N labeled APPTM WT and mutant peptide was directly dissolved in the following membrane mimic buffer systems: (A) 5% sodium dodecyl sulfate (SDS), 25 mM Sodium phosphate, pH 7.2; (B) 5% dodecylphosphocholine (DPC), 25 mM sodium phosphate, pH 7.2. Both buffers also contain 10% D₂O.

Determination of extinction coefficient of APPTM in micelles

After HPLC purification, APPTM in acetonitrile/water mix was divided into two equal parts. One part was sent to UCLA Biopolymer lab for quantitative amino acid analysis to get the total quantity of APPTM. The other half was lyophilized and dissolved in detergent micelles. Absorbance of APPTM in micelles at 220 nm was measured with a Nanodrop spectrophotometer (Thermo Scientific). According to Beer–Lambert law, $A = \varepsilon \ell c$, where A is absorbance, ε is the extinction coefficient, ℓ is the path length of light, and c is the concentration of the sample. We calculated the extinction coefficient of APPTM as $\varepsilon = A/\ell c$.

HSQC of APPTM

After reconstitution of APPTM into SDS and DPC, ¹⁵N–¹H HSQC of each sample was performed using a Bruker 800 MHz spectrometer equipped with a cryogenic probe, at 298 K, with an acquisition time of about 2 h. 4096 and 256 points were taken in the N and H dimensions, respectively. Spectrum widths are 12 ppm in the H dimension and 26 ppm in the N dimension, while centering at 4.7 ppm in the H dimension and 117 ppm in the N dimension. 16 total scans were used.

Results

Overexpression and purification of APPTM

The expression protocol of recombinant APPTM is shown in Fig. 1A. The expression level of the MBP-APPTM fusion protein

219

220

221

222

223

224

225

226

227

228

229

230

231

232

233

was induced by 1 mM IPTG followed by 24 h of growth at 30 °C (Fig. 1B). Clear differences can be observed on the SDS-PAGE gel between induced and uninduced cells. MBP-APPTM fusion protein (47 kDa) was the major product of the expression, accounting for about 70% of total protein, while it could not be detected without the addition of IPTG.

202

203

204

205

206

207

208

209

210

211

212

213

214

215

216

217

Purification procedures are also summarized in Fig. 1A. Cells were lysed by sonication in the presence of protease inhibitors. Fusion protein was purified from soluble fractions with Ni-NTA chromatography. Most of the impurities were in the flow-through while His-MBP-APPTM fusion protein was retained on the column. Target fusion protein appeared as the strongest band after Ni-NTA purification from SDS-PAGE gel (>90% purity) (Fig. 1C). At least 80% of the fusion protein was cleaved after incubation with TEV protease after 48 h (Fig. 1D, lane 1 and lane 2). APPTM was then further purified by RP-HPLC using a semi-preparative C4 column. A

40-90% acetonitrile gradient yielded an isolated APPTM peak (Fig. 2A). Since APPTM does not have any aromatic residues, it has no absorbance at 280 nm, but it generates strong signal at 220 nm due to absorbance by the peptide bonds. Therefore, the signature of APPTM in HPLC is the strong absorbance at 220 nm with no corresponding absorbance at 280 nm (Fig. 2A and B). The identity of the peptide was further confirmed by mass spectrometry (Fig. 2C). The appearance of an HPLC single peak and the small difference between measured mass (3231.947 Da) and theoretical mass (<0.1 Da) indicate the success of the purification strategy for APPTM. Purified APPTM was also verified by \$DS-PAGE gel (Fig. 2D). A single APPTM band indicates the high purity of the sample. Pure APPTM was then lyophilized and frozen at _→20 °C until further use. From 1] of LB culture, ~6 g of wet cells were harvested. ~160 mg of fusion protein were obtained after Ni-NTA affinity purification. The final yield of APPTM is about 2 mg. Using

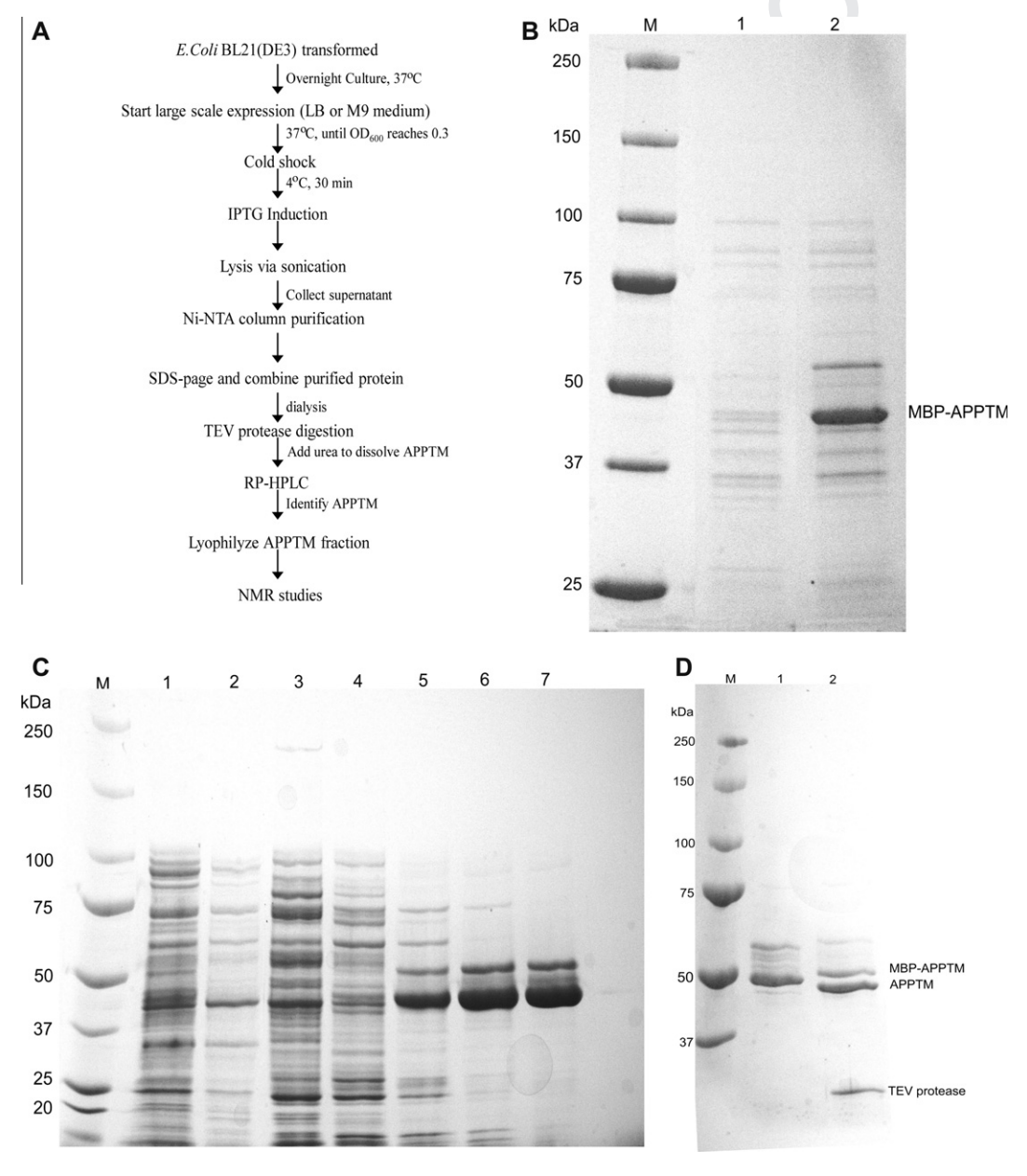


Fig. 1. Expression and purification of recombinant APPTM. (A) Flowchart for APPTM expression and purification. (B) SDS-PAGE of the samples before and after induction with IPTG. Lane M, molecular weight markers; lane 1, whole cell lysate uninduced; lane 2, cell lysate induced with 1 mM IPTG. (C) SDS-PAGE of the samples after Ni-NTA column chromatography. Lane 1, flowthrough of the lysate after injection through Ni-NTA column; lane 2, 3, 4, fractions that contains impurities separated by Ni-NTA purification; lane 5, 6, 7, relatively pure MBP-APPTM fusion protein after Ni-NTA chromatography. (D) SDS-PAGE of the TEV protease cleavage. Lane 1, fusion protein without addition of TEV protease; lane 2, 48 h after TEV protease cleavage.

W. Chen et al./Protein Expression and Purification xxx (2011) xxx-xxx

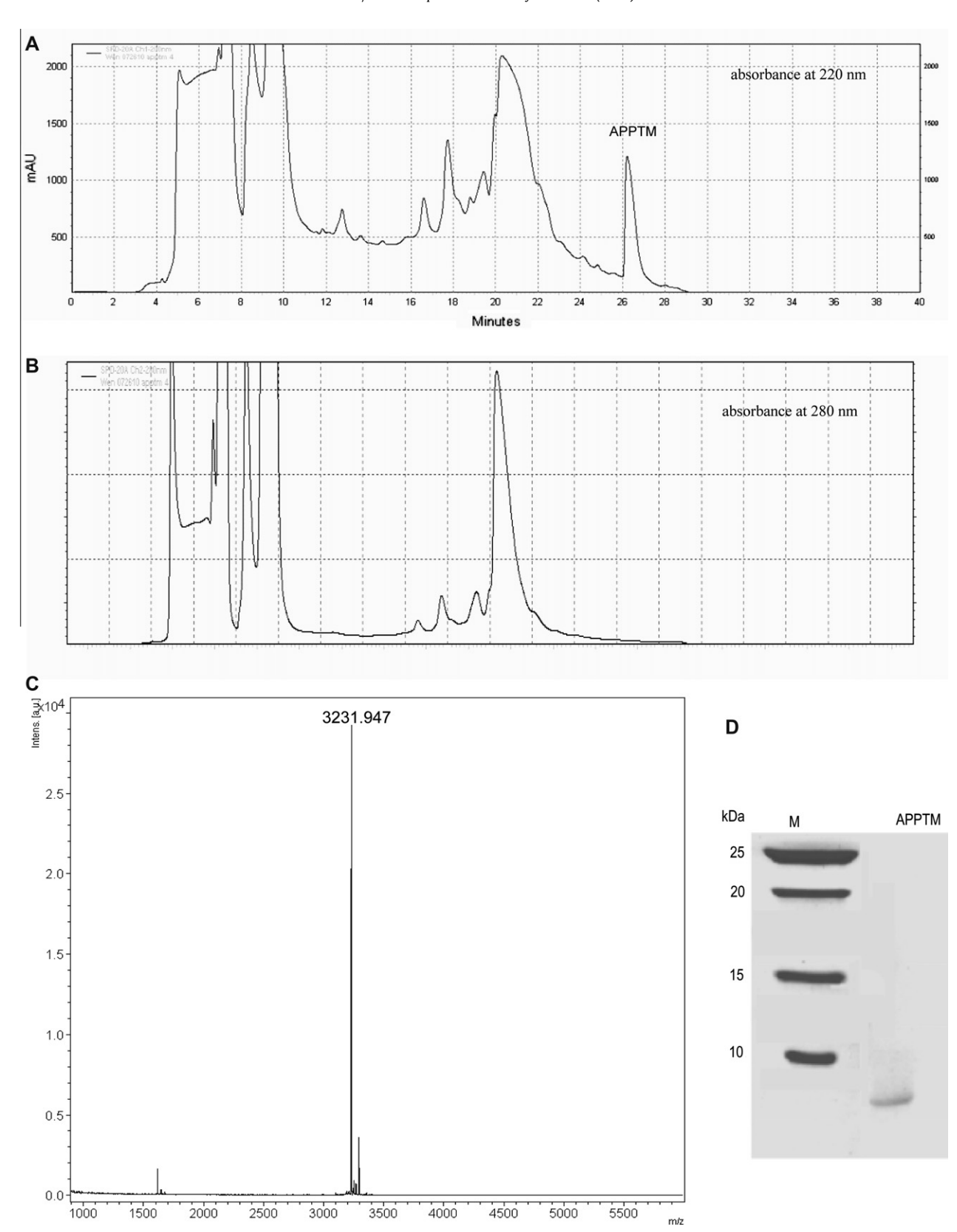


Fig. 2. HPLC purification and mass spectrometry validation of APPTM. (A) HPLC chromatogram of TEV digest mix, monitored at 220 nm. Single isolated APPTM peak appears at around 26 min. C4 column was used. (B) HPLC chromatogram of TEV digested mix, monitored at 280 nm. Due to the lack of aromatic residues in APPTM, no APPTM peak is observed. (C) Mass chromatogram of WT ¹⁵N labeled APPTM. Theoretical mass is 3231.87 Da while the actual measured mass is 3231.947 Da. (D) SDS-PAGE of pure APPTM after HPLC purification.

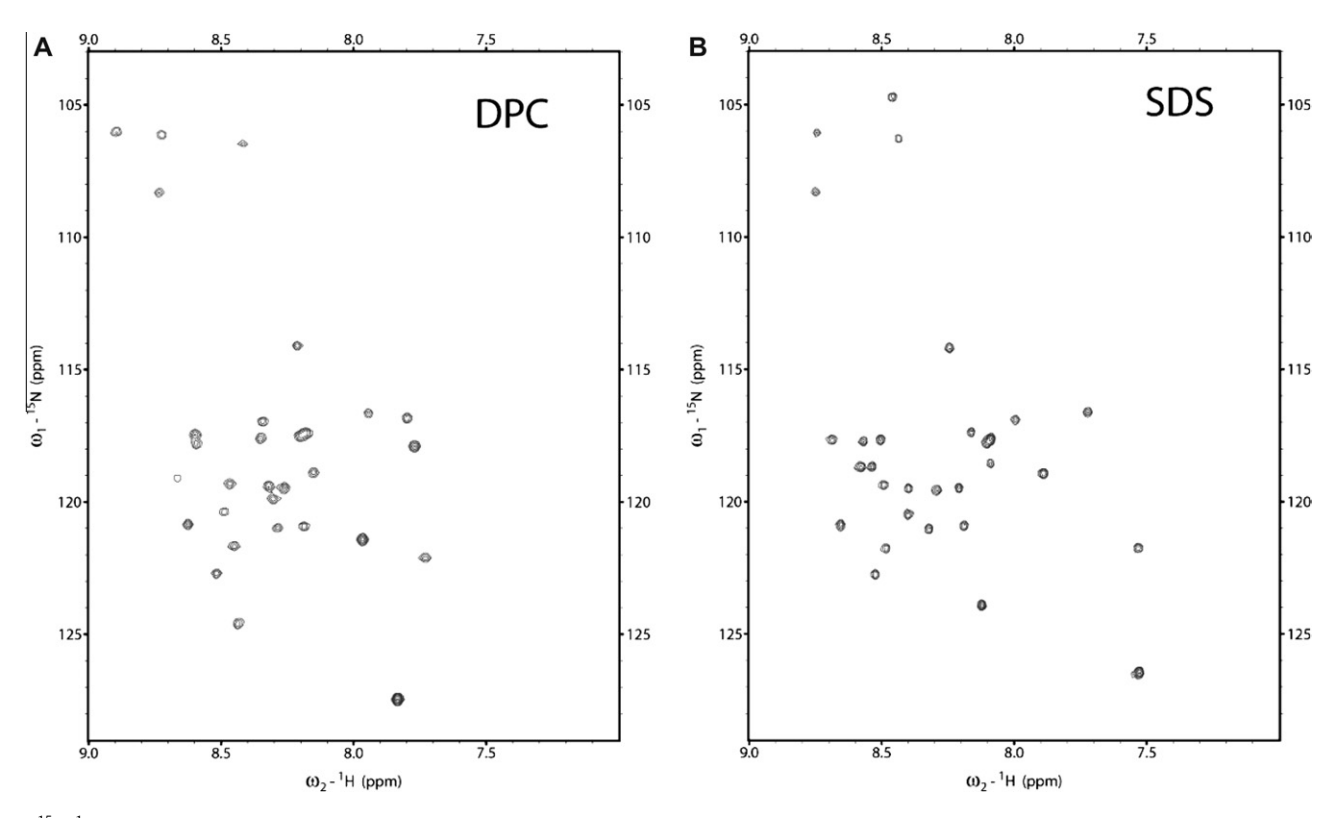


Fig. 3. ¹⁵N-¹H HSQC of APPTM in 5% DPC (A) and in 5% SDS (B). The sample concentration is approximately 0.1 mM. The NMR samples also contain 25 mM sodium phosphate buffer at pH 7.2 in 10% D₂O. APPTM has 32 residues. Thirty cross peaks are observed in both spectra, There are clear differences between HSQCs in DPC and SDS micelles.

M9 medium with 15 NH₄Cl, the 15 N labeled APPTM WT and V44M were also purified. The yield of 15 N labeled APPTM reaches ~ 50 –60% of natural abundant samples.

HSQC of APPTM in micelles

Detergent micelles are the most commonly used system for studying membrane protein structure. HSQC spectra were collected for APPTM in dodecylphosphocholine (DPC) and sodium dodecyl sulfate (SDS) micelles. Both spectra show excellent resolution and dispersion (Fig. 3). The recombinant APPTM has 32 residues. The first one or two residues of a protein or peptide are usually not detected due to fast solvent exchange. Thirty crosspeaks are observed in both spectra. However, significant chemical shift differences exist between the HSQCs in DPC and SDS, due to either conformational differences in APPTM or the difference in chemical environment between SDS and DPC micelles.

Determination of the extinction coefficient of APPTM in micelles

Due to the lack of aromatic residues of APPTM, concentration measurement by using absorbance at 280 nm does not work for APPTM. We used quantitative amino acid analysis (AAA) in combination with Nanodrop spectrophotometric measurement to estimate the extinction coefficient of APPTM at 220 nm. Quantitative AAA revealed the total mass of APPTM in a sample, from which the concentration was calculated. We determined the value of the extinction coefficient of APPTM at 220 nm is 94.62 mM⁻¹ cm⁻¹.

HSQC of APPTM WT and V44M in DPC

HSQC data for APPTM WT and V44M were both acquired in DPC (Fig. 4). There are obvious differences in peak position, indicating the effect of the V44M mutant on APPTM structure.

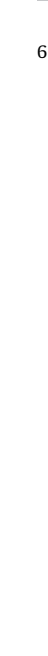
Discussion

Despite the importance of APPTM in the production of Aβ and the mechanism of Alzheimer's disease, there is no experimental structure of APPTM at atomic resolution. NMR sample preparation is the first step for determining APPTM structure. Membrane proteins are inherently difficult to express and solubilize in aqueous solution due to their extremely hydrophobic nature. To resolve this problem, we used the MBP fusion to enhance the expression level and solubility of the expressed protein. Alternatively, ketosteroid isomerase (KSI) fusion protein can also be successfully used for overexpressing APPTM [18,19].

For TEV protease digestion, high concentration of the MBP-APPTM fusion protein usually resulted in poor cleavage (less than 40%, data not shown). This is probably because hydrophobic APPTM tends to aggregate at higher concentrations, possibly hindering the interaction between TEV protease and its recognition site. Relatively lower concentration of fusion protein (<3 mg/ml), plus at least 48 h of digestion on a Nutator consistently yields more than 80% digestion of the total fusion protein.

After TEV protease cleavage, we tried to use Ni-NTA column again to remove digested and undigested MBP-APPTM from APPTM. However, the strongly hydrophobic APPTM can not be completely separated from fusion proteins by Ni-NTA column, even with the presence of 8 M urea. APPTM tends to stick to MBP or nickel beads because of its strong hydrophobic character. The digestion mixture was therefore applied directly to RP C4 column without further Ni-NTA processing.

Pure APPTM can be separated from the digestion mixture using a water/acetonitrile gradient on a C4 reverse phase HPLC column. This step can be time consuming because of the concentration limit of the digestion and the injection volume limit of the HPLC. Multiple injections are necessary for a high quality NMR sample. APPTM likely precipitate at low acetonitrile concentrations in the column, causing the fast deterioration of the column performance.



297

298

299

300

301

302

303

304

305 306

307 308

309

310

311

312

313

314

315

316

317

318

319

320

321

322

323

324

325

326

327

328

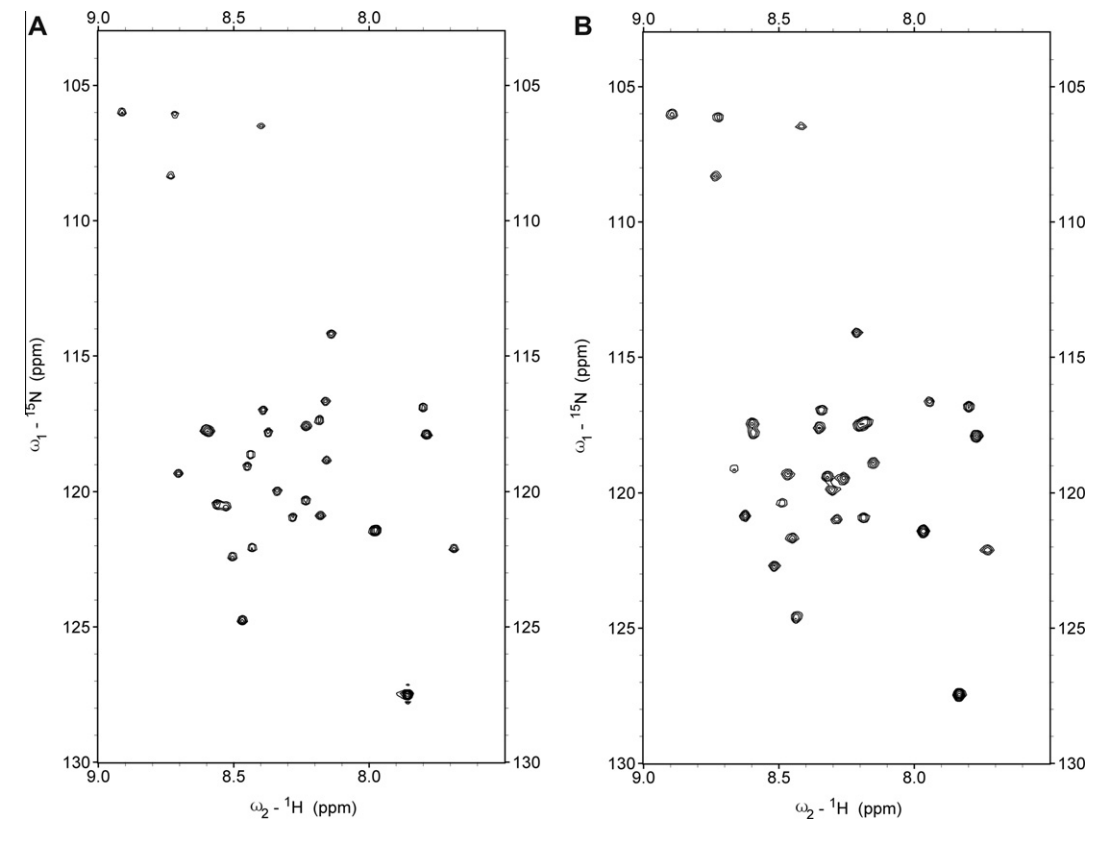


Fig. 4. ¹⁵N-¹H HSQC of APPTM WT (A) and APPTM V44M (B) in DPC micelles. WT and V44M display different HSQC patterns, suggesting their different local conformation caused by mutation.

Another possible method to purify APPTM is to use Hydrophilic-Interaction Chromatography (HILIC). When eluting HILIC columns with hydrophobic mobile phase, solutes with higher hydrophilicity have longer retention time [20]. This can avoid the precipitation of membrane proteins onto RP HPLC columns and frequent column cleaning. Cell-free expression is also an alternative method to produce APPTM. It enables membrane protein translation directly into detergent micelles or into precipitates which can be easily purified [21]. ¹⁵N-and/or ¹³C-labeled protein can also be produced using a cell-free system.

It is crucial to test a variety of sample conditions to obtain optimal dispersion and resolution of the NMR spectra of APPTM. Detergent micelles are the most frequently used system for studying membrane proteins. In the literature, there are several detergents that can provide high quality NMR spectra, such as SDS, DPC, Sarcosyl, 1-palmitoyl-2-hydroxy-sn-glycero-3-[phospho-RAC-(1glycerol)] (LPPG), 1-myristoyl-2-hydroxy-sn-glycero-3-[phospho-RAC-(1-glycerol)] (LMPG), N,N-dimethyldodecylamine N-oxide (LDAO), *n*-octyl-β-D-glucopyranoside (βOG), *n*-dodecyl-β-D-maltoside (DM) and 1,2-dicaproyl-1-sn-glycero-3-[phospho-RAC-(1glycerol)] (DHPC) [22-25]. SDS and DPC were tested first. They both provided HSQC spectra with excellent dispersion and resolution. In most cases, the zwitterionic DPC is expected to be less denaturing than the anionic SDS. It has been shown that DPC can preserve the native conformations of membrane peptides and enzyme activity of membrane proteins [26,27].

Lipid environment is also very important for APP processing. Lu et al. [28] showed that the dynamics of APPTM helix change with different types of lipids using solid-state NMR. Beel et al. [13] showed the association of APP with cholesterol with solution NMR. Evidence in the literature suggests that γ -secretase processing of APP occurs in lipid rafts in *in vivo* [29–31]. In addition, the structural properties of other membrane proteins such as

voltage-sensor domains (VSDs) are dependent on the lipid environment [32]. Therefore, in addition to SDS and DPC micelle, lipid-containing membrane mimetics, such as lipid bilayer and bicelles, will be tested for NMR studies of APPTM.

In summary, we have developed an effective and reliable method to purify both WT and mutant recombinant APPTM. It lays a good foundation for NMR structural and functional studies of APPTM, and, for the better understanding of A β production and Alzheimer's disease.

Acknowledgments

We are grateful for the financial support from American Health Assistance Foundation (A2009340). We thank European Molecular Biology Laboratory for providing the pETM41 vector.

References

- [1] D.J. Selkoe, Alzheimer's disease: genes, proteins, and therapy, Physiol. Rev. 81 (2) (2001) 741–766.
- [2] J. Hardy, D.J. Selkoe, The amyloid hypothesis of Alzheimer's disease: progress and problems on the road to therapeutics, Science 297 (5580) (2002) 353–356.
- [3] D.J. Selkoe, Toward a comprehensive theory for Alzheimer's disease. Hypothesis: Alzheimer's disease is caused by the cerebral accumulation and cytotoxicity of amyloid beta-protein, Ann. NY Acad. Sci. 924 (2000) 17–25.
- [4] D. Burdick et al., Assembly and aggregation properties of synthetic Alzheimer's A4/beta amyloid peptide analogs, J. Biol. Chem. 267 (1) (1992) 546-554.
- 5] W. Annaert, B. De Strooper, A cell biological perspective on Alzheimer's disease, Annu. Rev. Cell Dev. Biol. 18 (2002) 25–51.
- [6] S. Sinha et al., Purification and cloning of amyloid precursor protein betasecretase from human brain, Nature 402 (6761) (1999) 537–540.
- [7] R. Vassar et al., Beta-secretase cleavage of Alzheimer's amyloid precursor protein by the transmembrane aspartic protease BACE, Science 286 (5440) (1999) 735–741.
- [8] P.C. Fraering et al., Purification and characterization of the human gammasecretase complex, Biochemistry 43 (30) (2004) 9774–9789.

329

330

336 337

339 340 341

338

341

393 394

264 (5163) (1994) 1336-1340. [12] M.H. Scheinfeld et al., Jun NH2-terminal kinase (JNK) interacting protein 1

(JIP1) binds the cytoplasmic domain of the Alzheimer's beta-amyloid precursor protein (APP), J. Biol. Chem. 277 (5) (2002) 3767-3775 [13] A.J. Beel et al., Structural studies of the transmembrane C-terminal domain of the amyloid precursor protein (APP): does APP function as a cholesterol sensor? Biochemistry 47 (36) (2008) 9428-9446. [14] T. Sato et al., A helix-to-coil transition at the epsilon-cut site in the

transmembrane dimer of the amyloid precursor protein is required for proteolysis, Proc. Natl. Acad. Sci. USA 106 (5) (2009) 1421-1426. [15] N. Miyashita et al., Transmembrane structures of amyloid precursor protein

[9] C. Haass, Take five-BACE and the gamma-secretase quartet conduct

[10] M.E. Fortini, Gamma-secretase-mediated proteolysis in cell-surface-receptor

[11] N. Suzuki et al., An increased percentage of long amyloid beta protein secreted

signalling, Nat. Rev. Mol. Cell Biol. 3 (9) (2002) 673-684.

Alzheimer's amyloid beta-peptide generation, EMBO J. 23 (3) (2004) 483-488.

by familial amyloid beta protein precursor (beta APP717) mutants, Science

dimer predicted by replica-exchange molecular dynamics simulations, J. Am. Chem. Soc. 131 (10) (2009) 3438-3439.

[16] H. Wang et al., Molecular determinants and thermodynamics of the amyloid precursor protein transmembrane domain implicated in Alzheimer's disease, J. Mol. Biol. 408 (5) (2011) 879-895.

[17] Y.I. Yin et al., {gamma}-Secretase substrate concentration modulates the Abeta42/Abeta40 ratio: implications for Alzheimer disease, J. Biol. Chem. 282 (32) (2007) 23639-23644.

[18] O.V. Bocharova et al., Expression and purification of a recombinant transmembrane domain amyloid precursor protein associated with Alzheimer's disease, Bioorg. Khim. 36 (1) (2010) 105-111.

[19] T.J. Park et al., Optimization of expression, purification, and NMR measurement for structural studies of transmembrane region of amyloid beta protein, Biotechnol. Bioprocess Eng. 16 (3) (2011) 477-481.

[20] A.J. Alpert, Hydrophilic-interaction chromatography for the separation of peptides nucleic acids and other polar compounds, J. Chromatogr. 499 (1990) [21] B. Schneider et al., Membrane protein expression in cell-free systems, Methods Mol. Biol. 601 (2010) 165-186.

[22] L. Columbus et al., Expression, purification, and characterization of Thermotoga maritima membrane proteins for structure determination, Protein Sci. 15 (5) (2006) 961-975.

[23] R.D. Krueger-Koplin et al., An evaluation of detergents for NMR structural studies of membrane proteins, J. Biomol. NMR 28 (1) (2004) 43-57.

[24] R.C. Page et al., Comprehensive evaluation of solution nuclear magnetic resonance spectroscopy sample preparation for helical integral membrane proteins, J. Struct. Funct. Genomics 7 (1) (2006) 51-64.

S.F. Poget, M.E. Girvin, Solution NMR of membrane proteins in bilayer mimics: small is beautiful, but sometimes bigger is better, Biochim. Biophys. Acta 1768 (12) (2007) 3098-3106.

[26] F. Porcelli et al., Structures of the dimeric and monomeric variants of magainin antimicrobial peptides (MSI-78 and MSI-594) in micelles and bilayers, determined by NMR spectroscopy, Biochemistry 45 (18) (2006) 5793-5799.

[27] F. Porcelli et al., NMR structure of the cathelicidin-derived human antimicrobial peptide LL-37 in dodecylphosphocholine Biochemistry 47 (20) (2008) 5565–5572.

[28] J.X. Lu, W.M. Yau, R. Tycko, Evidence from solid-state NMR for nonhelical conformations in the transmembrane domain of the amyloid precursor protein, Biophys. J. 100 (3) (2011) 711-719.

[29] R. Ehehalt et al., Amyloidogenic processing of the Alzheimer betaamyloid precursor protein depends on lipid rafts, J. Cell Biol. 160 (1) (2003) 113-123.

[30] K.S. Vetrivel et al., Association of gamma-secretase with lipid rafts in post-golgi and endosome membranes, J. Biol. Chem. 279 (43) (2004) 44945-44954.

[31] P. Osenkowski et al., Direct and potent regulation of gamma-secretase by its lipid microenvironment, J. Biol. Chem. 283 (33) (2008) 22529-22540.

[32] J.A. Butterwick, R. MacKinnon, Solution structure and phospholipid interactions of the isolated voltage-sensor domain from KvAP, J. Mol. Biol. 403 (4) (2010) 591-606.

7

395

396

397

398

399

400

401

402

403

404

405

406

407

408

409

410

411

412 413

414

415

416

417

418

419

420

421

422

427 428